



# The Use of *Saccharum Officinarum* Bagasse and Chicken Eggshells to Synthesize Calcium Silicates

Anti Kolonial Prodjosantoso<sup>(✉)</sup>, Yoga Putri Rahmawati, Kun Sri Budiasih, and Dyah Purwaningsih

Chemistry Department, Yogyakarta State University, Yogyakarta 55281, Indonesia  
prodjosantoso@uny.ac.id

**Abstract.** Calcium silicate is one of the cement components that can be synthesized by using calcium oxide (CaO) and silica (SiO<sub>2</sub>) derived from limestone and sand, respectively. The precursors used to synthesize calcium silicate are extracted by mining which may damage the environment. The purpose of this study was to synthesize calcium silicate compounds by replacing limestone and clay with organic materials to reduce environmental problems.

Potential precursors to the synthesis of calcium silicate compounds are broiler chicken eggshells and green sugarcane wastes. Calcined broiler chicken eggshells contain mainly solid calcium oxide (80% of CaO), and the calcined bagasse contains 66.70% of silica (SiO<sub>2</sub>). In this study, broiler chicken eggshells were calcined at 800 °C for 10 h to decompose calcium carbonate (CaCO<sub>3</sub>) to calcium oxide (CaO), while bagasse was calcined at 800 °C for 4 h to produce silica (SiO<sub>2</sub>).

Calcium silicate was synthesized using the solid-state reaction method of stoichiometric mixtures of calcium oxide (CaO) dan silica (SiO<sub>2</sub>) at a varied temperature of 950 °C, 1000 °C, and 1050 °C. The calcined products were characterized using XRD, FTIR, TGA-DSC, and SEM-EDX methods. In general, the samples contain two main phases of calcium silicate, namely Ca<sub>2</sub>SiO<sub>4</sub> (larnite) and Ca<sub>3</sub>SiO<sub>5</sub> (alite). The mole percentage of calcium silicate increases with the increasing synthesis temperature and the calcined broiler chicken eggshell used as a precursor.

**Keywords:** calcium silicate · SiO<sub>2</sub> · CaO · calcination

## 1 Introduction

Human activities produce wastes, both organic and inorganic waste. Organic waste is mainly household waste. The untreated waste results in a negative impact on the environment (Hasibuan, 2016). One of the waste is broiler egg shells. Indonesia is able to produce 4,753,382 tons of eggs to meet the needs of the community, and the released eggshells cause new environmental problems. However, the main content of eggshells is calcium carbonate (CaCO<sub>3</sub>), and the minor of phosphorus (0.12%), sodium (0.15–0.17%), magnesium (0.37–0.40%), potassium (0.10–0.13%), sulfur (0.09–0.19%), as

well as various other organic compounds such as protein, fat, alanine, and arginine (Warsy and S. Chadijah, 2016).

In addition, bagasse is also a relatively large contributor to organic waste. Purnawan et al. (2018) stated that bagasse is rich in compounds that might be used as new products, because the ash of bagasse contains compounds which include  $\text{SiO}_2$  (66.70%),  $\text{K}_2\text{O}$  (9.05%),  $\text{CaO}$  (8.14%),  $\text{Fe}_2\text{O}_3$  (4.76%),  $\text{Al}_2\text{O}_3$  (4.21%),  $\text{MgO}$  (3.06%), and  $\text{P}_2\text{O}_5$  (2.35%).

Calcium silicate is a cement composition that contributes greatly to providing compressive strength in cement (Ningsih et al., 2012). There are many types of calcium silicate, including dicalcium silicate ( $\text{Ca}_2\text{SiO}_4$ ) in the form of  $\alpha$ -dicalcium silicate ( $\alpha\text{-C}_2\text{S}$ ) (Kriskova et al., 2014),  $\beta$ -dicalcium silicate ( $\beta\text{-C}_2\text{S}$ ), and  $\gamma$ -dicalcium silicate ( $\gamma\text{-C}_2\text{S}$ ) (Liu et al., 2019), and tricalcium silicate ( $\text{Ca}_3\text{SiO}_5$ ) and many other types. Synthesis of calcium silicate compounds usually produces many types but the dominant one is dicalcium silicate (Nicoleau et al., 2013). This is because dicalcium silicate compounds can be synthesized using the solids reaction method at a temperature of  $950^\circ\text{C}$  (Haryono and Eddy et al., 2018) compared to tricalcium silicate ( $\text{Ca}_3\text{SiO}_5$ ) which requires a higher synthesis temperature (Nicoleau et al., 2013).

Calcium silicate compounds can be synthesized using precursors of calcium oxide ( $\text{CaO}$ ) or limestone and silica ( $\text{SiO}_2$ ) sourced from clay (Yenny, 2011). Calcium oxide ( $\text{CaO}$ ) and silica ( $\text{SiO}_2$ ) are produced through the mining process. The mining activities include demolition and land clearing. These kinds of activities can cause environmental changes such as changes in soil morphology, changes in land use, causes land slopes, and even reducing groundwater by up to 72% (Khristian, 2014).

In this research, the synthesis of calcium silicate compounds will be carried out by utilizing waste from eggshells to obtain calcium oxide ( $\text{CaO}$ ) and bagasse as a source of silica ( $\text{SiO}_2$ ). The research also looked for an optimum variable to produce calcium silicate using calcium oxide ( $\text{CaO}$ ) and silica ( $\text{SiO}_2$ ) as precursors? This research output is expected to help reduce environmental problems, including the mining problems in cement production.

## 2 Experimental

The type of eggshell used in this study was Broiler egg shell taken from martabak traders in Condongcatur, Sleman, while the bagasse waste was collected from green sugarcane juice sellers in Caturtunggal, Sleman.

The resulting calcium silicate compounds were characterized by using a series of methods. XRD (X-Ray Diffraction) type of Bruker D2 Phaser diffractometer was operated monochromatic  $\text{Cu K}\alpha$  radiation with a wavelength ( $\lambda$ ) of 1.54184 in the range of  $2\theta$  between  $2^\circ$  to  $90^\circ$ . FTIR (Fourier Transform Infra-Red) type Nicolet iS5 was used to detect and identify peaks from the analyzed sample spectra in order to investigate the functional groups of compounds contained in the sample. SEM-EDX (Scanning Electron Microscope-Energy Dispersive X-Ray) type JEOL JSM-6510LA was used to study the surface morphology of the sample and determine the elements contained and the amount in the sample.

Syntheses of calcium silicate compounds were conducted as follows.

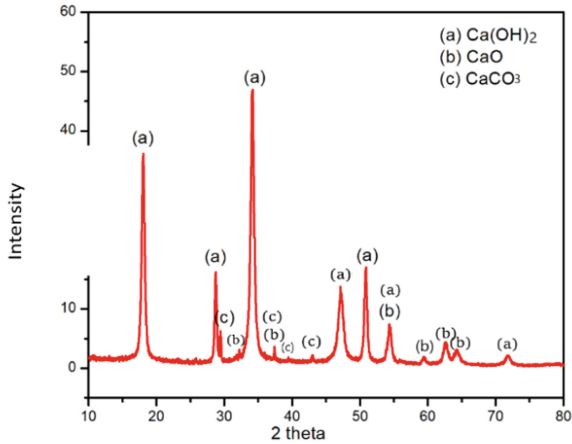


Fig. 1. The XRD pattern of the broiler eggshell ash.

- a. The sample was synthesized by mixing broiler eggshell ash and green bagasse ash in a mole ratio of 2.1:1 (mixture code: 2110) and put into a porcelain mortar. The mixture was ground until homogeneous by adding acetone. The mixture was then transferred to a crucible.
- b. The mixture was heated using a muffle furnace at a temperature of 950 °C for four hours followed by air quenching (sample code: 2110-950).
- c. Steps a and b were carried out for broiler eggshell ash and green bagasse ash mixture in a mole ratio of 2:1 and 1.9:1.
- d. The mixture with a mole ratio of 2:1 was calcined at 950 °C, 1000 °C, and 1050 °C, with the sample names are 2010-950, 2010-1000, and 2010-1050, respectively. Meanwhile, the mixtures of mole ratios of 1.9:1 and 2.1:1 were calcined at 950 °C, and the samples were coded as 1910-950 and 2110-950, respectively.

### 3 Results and Discussion

#### X-Ray Diffraction (XRD) Method

XRD analysis was performed using a Bruker D2 Phaser diffractometer using a monochromatic Cu K $\alpha$  radiation with a wavelength ( $\lambda$ ) of 1.54184 in the range of  $2\theta$  between 10° to 80°. The diffraction patterns of each sample indicate the phases in the sample.

The XRD pattern of the broiler eggshell ash (Fig. 1) was analyzed using the Origin application and the data was compared with JCPDS. Figure 1 indicates the presence of Ca(OH)<sub>2</sub>, CaO, and CaCO<sub>3</sub> in the sample. The specific peaks at  $2\theta = 33.045^\circ$ ,  $37.379^\circ$ ,  $54.348^\circ$ ,  $59.394^\circ$ ,  $64.284^\circ$ , and  $64.626^\circ$  indicate CaO (JCPDS no. 00-037-1497). The peaks at  $2\theta = 18.059^\circ$ ,  $28.726^\circ$ ,  $34.151^\circ$ ,  $47.202^\circ$ ,  $50.861^\circ$ ,  $54.348^\circ$ , and  $71.806^\circ$  corresponds to JCPDS no. 01-073-5492 for Ca(OH)<sub>2</sub>. Low and non-dominant peaks are identified at  $2\theta = 29.444^\circ$ ,  $37.379^\circ$ ,  $39,458^\circ$ , and  $42,961^\circ$  according to JCPDS no. 085-1108 for CaCO<sub>3</sub>.

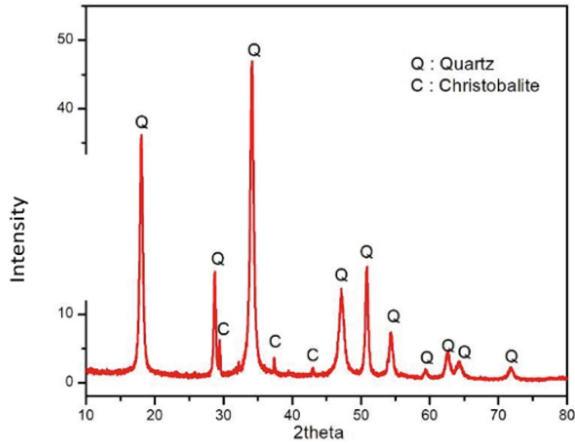
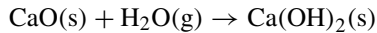


**Fig. 2.** XRD pattern of the green bagasse ash.

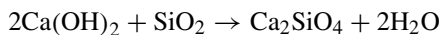
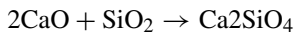
A quantitative analysis using the Match 3.0 program reveals that the content of  $\text{Ca(OH)}_2$ ,  $\text{CaO}$  and  $\text{CaCO}_3$  in the sample are 52.7%, 35.4% and 11.9% respectively. The dominant amount of  $\text{Ca(OH)}_2$  in the sample is produced by the reaction of  $\text{CaO}$  to water vapor in the air during the cooling process of the sample. The hydration process of  $\text{CaO}$  follows the reaction belows.



On the other hand, the evidence collected using TGA-DSC indicates the  $\text{CaCO}_3$  contained in egg shells has not been completely decomposed.

The diffraction pattern of the green bagasse ash is ascribed in Fig. 2. According to Soares et al. (2014) the peaks at about  $2\theta = \sim 20^\circ$ ,  $\sim 18^\circ$ ,  $\sim 29^\circ$ ,  $\sim 34\text{--}35^\circ$ ,  $\sim 43\text{--}44^\circ$ ,  $\sim 50^\circ$ , and  $\sim 53^\circ$  are typical peaks of quartz  $\text{SiO}_2$  phase, while the peaks at about  $2\theta = \sim 30^\circ$ ,  $\sim 38^\circ$ , and  $\sim 43^\circ$  are the christobalite  $\text{SiO}_2$  phase. In this study, we identify a quartz phase of  $\text{SiO}_2$ , indicated by  $18.904^\circ$ ,  $29.173^\circ$ ,  $34.601^\circ$ ,  $43.640^\circ$ ,  $50.393^\circ$  and  $53.984^\circ$ . The christobalite peaks at  $2\theta = 30.415^\circ$ ,  $38.094^\circ$  and  $43.460^\circ$  are also identified. An analysis using Match 3.0 indicates the quartz phase (90.1%) and the christobalite (9.9%).

The samples 1910-950, 2010-950, 2110-950, 2010-1000, 2010-1050 consist of various phases (Tables 1 and 2). The main phase of the samples is  $\text{Ca}_2\text{SiO}_4$  (larnite), with another minor phase  $\text{Ca}_3\text{SiO}_5$  (alite). The  $\text{Ca}_2\text{SiO}_4$  (larnite) and  $\text{Ca}_3\text{SiO}_5$  (alite) are formed by the reaction between  $\text{SiO}_2$  and  $\text{Ca(OH)}_2$  as follows.



As expected, the phases of calcium silicates are very dominant in the samples (Table 1). The more broiler eggshell ash added to the green bagasse ash, the more  $\text{Ca(OH)}_2$  and  $\text{CaO}$  content in the samples, and the amount of  $\text{Ca}_3\text{SiO}_5$  (alite) in the samples are decreasing.

**Table 1.** The mole percentage of phases in the samples prepared at 950 °C.

Phases	Mole percentage (%)		
	1910-950	2010-950	2110-950
Ca <sub>2</sub> SiO <sub>4</sub> ( <i>larnite</i> )	42.1	46.9	52.3
Ca <sub>3</sub> SiO <sub>5</sub> ( <i>alite</i> )	24.8	24.0	16.5
SiO <sub>2</sub>	11.9	6.8	6.7
Ca(OH) <sub>2</sub>	14.3	15.0	16.4
CaO	6.9	7.4	8.1

**Table 2.** The mole percentage of phases in the samples prepared at 950 °C, 1000 °C dan 1050 °C.

Phases	Mole percentage (%)		
	2010-950	2010-1000	2010-1050
Ca <sub>2</sub> SiO <sub>4</sub> ( <i>larnite</i> )	46.9	48.5	51.7
Ca <sub>3</sub> SiO <sub>5</sub> ( <i>alite</i> )	24.0	27.7	24.6
SiO <sub>2</sub>	6.8	5.3	5.3
Ca(OH) <sub>2</sub>	15.0	10.9	10.8
CaO	7.4	7.6	7.5

This finding agrees with that of Haryono. E, et al. (2018) who stated that the most dominant calcium silicate compound was Ca<sub>2</sub>SiO<sub>4</sub> (*larnite*). Because of its dominant nature, in the synthesis of calcium silicate, Ca<sub>2</sub>SiO<sub>4</sub> (*larnite*) will be formed first than Ca<sub>3</sub>SiO<sub>5</sub> (*alite*). In addition, Haryono. E, et al. (2018) explained that at the same synthesis temperature of 950 °C Ca<sub>2</sub>SiO<sub>4</sub> (*larnite*) was more abundant than Ca<sub>3</sub>SiO<sub>5</sub> (*alite*).

The amount of Ca<sub>2</sub>SiO<sub>4</sub> (*larnite*) and Ca<sub>3</sub>SiO<sub>5</sub> (*alite*) phases in the samples is increased with the increasing synthesis temperature, while the amount of SiO<sub>2</sub> and Ca(OH)<sub>2</sub> is decreased (Table 2). This indicates that the reaction between SiO<sub>2</sub> and Ca(OH)<sub>2</sub> is well undertaken, resulting in the production of Ca<sub>2</sub>SiO<sub>4</sub> (*larnite*) and Ca<sub>3</sub>SiO<sub>5</sub> (*alite*) which are mostly found in the 2010-1050 sample. The high calcination temperature causes the reaction between Ca(OH)<sub>2</sub> and SiO<sub>2</sub> is maximized. If the reaction is carried out with a combination of repeated grinding, the reaction will run perfectly and more Ca<sub>2</sub>SiO<sub>4</sub> (*larnite*) and Ca<sub>3</sub>SiO<sub>5</sub> (*alite*) are obtained.

The data tabulated in Tables 1 and 2 are in accordance with Haryono's explanation (2018) who explained that Ca<sub>2</sub>SiO<sub>4</sub> (*larnite*) and Ca<sub>3</sub>SiO<sub>5</sub> (*alite*) were successfully synthesized at a temperature of 950 °C with the amount of Ca<sub>2</sub>SiO<sub>4</sub> (*larnite*) is more dominant. Practically, the Ca(OH)<sub>2</sub> in the sample will be stabilized by Ca<sub>2</sub>SiO<sub>4</sub> (*larnite*) and Ca<sub>3</sub>SiO<sub>5</sub> (*alite*) in the cement, making the structures are stronger and more compact.

The XRD diffractogram of all samples in this study can be seen in Fig. 3. The diffraction pattern shows a similar peak position, and the pattern also explains the presence of

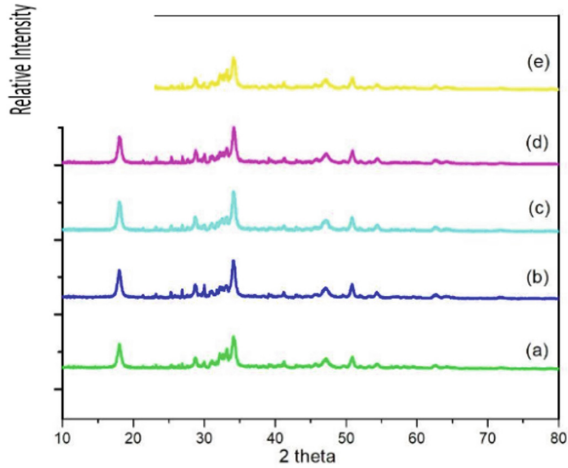


**Fig. 3.** XRD pattern of 1910-950 (a), 2010-950 (b), 2110-950 (c), 2010-1000 (d), and 2010-1050 (e) samples.

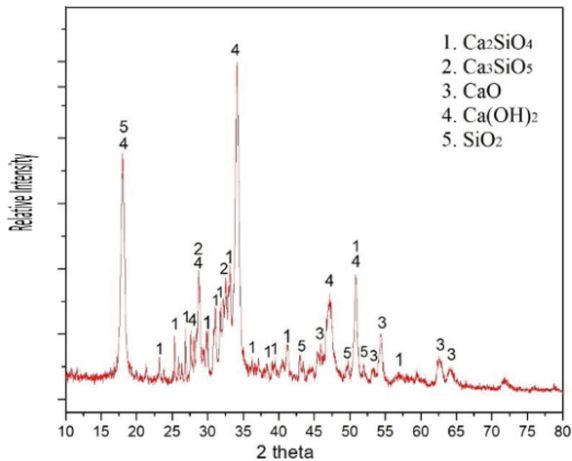


**Fig. 4.** XRD pattern of 1910-950 sample.

a typical peak of a compound contained in the sample. The XRD diffraction pattern of 1910-950 sample (Fig. 4) indicates a small and low peak at around  $25^{\circ}$  to  $37^{\circ}$  which is increased with the increase of the amount of broiler eggshell ash precursor in the 2010-950 and 2110-950 samples. Meanwhile, in the 2010-1000 and 2010-1050 samples, the small peak disappeared again with increasing calcination temperature. Comparing the diffraction pattern of the samples which the JCPDS data result in a conclusion that four compounds are contained in the sample, namely  $\text{Ca}_2\text{SiO}_4$  (Iarnite),  $\text{Ca}_3\text{SiO}_5$  (alite),  $\text{Ca}(\text{OH})_2$ , and  $\text{SiO}_2$ .

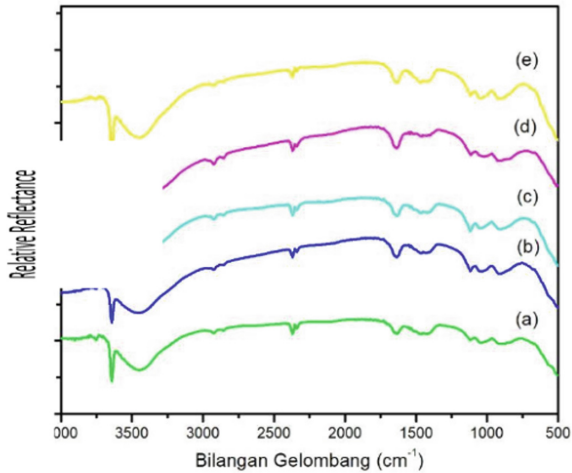


**Fig. 5.** FTIR spectrum of sample 1910-950 (a), 2010-950 (b), 2010-1000 (c), 2010-1050 (d), dan 2110-950 (e).

### Infrared Spectroscopy Method

Samples testing using the infrared spectroscopy method is intended to determine the functional groups and vibrational spectrum contained in the samples under study. The instrument used for the analysis is the Fourier Transform Infra-Red (FTIR) Nicolet iS5 type. The spectra of all compounds produce peaks that are almost similar to each other. The analysis starts from the wavelength of 500–4000  $\text{cm}^{-1}$  for all samples.

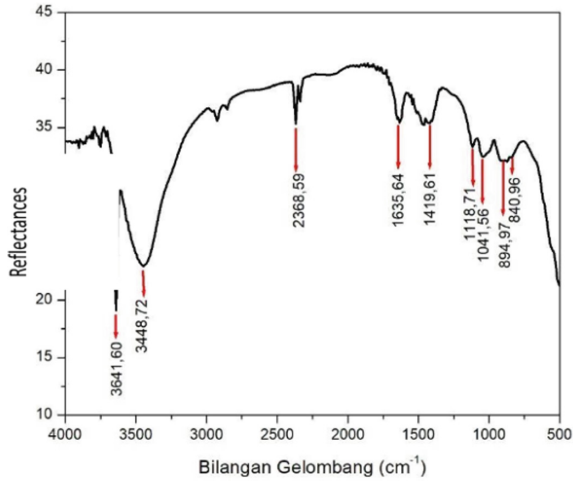
Figure 5 shows the presence of several wavenumber absorption bands which are almost the same in all samples. O–H bending and O–H stretching vibrations give a widening peak in all samples so as to produce wavenumbers that are relatively the same in all samples.

Figure 6 depicts the spectrum and wavelength of samples 1910-950. The band at the  $\sim 840.96 \text{ cm}^{-1}$  indicates an O–Si–O symmetric stretching bond, and in the  $\sim 894.97 \text{ cm}^{-1}$  is a Si–O–Ca bond, and in the  $\sim 1041.56 \text{ cm}^{-1}$  and  $1118.71 \text{ cm}^{-1}$  are detected as asymmetric stretching Si–O–Si bonds. The bending OH bond originating from  $\text{Ca}(\text{OH})_2$  is detected in the  $\sim 1635.64 \text{ cm}^{-1}$ , and a very sharp peak in the  $\sim 2368.59 \text{ cm}^{-1}$  is detected as a C = O bond from  $\text{CO}_2$ , the stretching OH bond is detected in two regions, namely  $\sim 3448.72 \text{ cm}^{-1}$  and  $\sim 3641.60 \text{ cm}^{-1}$ , while asymmetric stretching CO bond is detected in the  $\sim 1419.61 \text{ cm}^{-1}$ .

### Scanning Electronic Microscope Elektron Dispersive X-Ray Analyser (SEM-EDX) Method

The SEM method combined with EDX was employed to investigate the examined samples' elemental composition and interfacial properties. The SEM-EDX instrument used is the SEM-EDX type JEOL JSM-6510LA. Analysis using SEM-EDX method was carried out for samples 1910-950, 2010-950, 2110-950, 2010-1000, 2010-1050.

The morphology of all calcium silicate samples is similar. All samples are crystalline with various surface morphologies. Samples 1910-950 and 2010-1050 has tapered ends



**Fig. 6.** FTIR spectrum of sample 1910–950.

like rods, while the other samples has blunt ends. The surface of all samples is smooth, but the sample 2110-950 looks a little rough, compared to the other sample surfaces. In addition, the particle distribution of all samples tends to be heterogeneous. The morphology of the samples is shown in Fig. 7.

The elemental content in each sample tends to vary. The main elements contained in the samples are Si and Ca. The presence of the elements in the sample is indicated in the EDX spectra (Fig. 8).

Based on the EDX spectra (Fig. 8), the Ca (89,001% mole) is observed as the main element in the sample 1910-950, while the Si (5404% mole) is in the sample 2010-1000. In all samples, there are other minor elements (Table 3). The results of the EDX analysis cannot be used as a reference for the number of atoms contained in the samples because the analysis is carried out only on certain surface areas, and so the results are irrelevant when used as a reference.

## 4 Conclusions

The calcium silicates can be synthesized from the organic waste, namely broiler eggshell as a source of calcium oxide (CaO) and green bagasse (*Saccharum officinarum*) as a source of silica (SiO<sub>2</sub>). The calcium silicates that were successfully synthesized are Ca<sub>2</sub>SiO<sub>4</sub> (larnite) and Ca<sub>3</sub>SiO<sub>5</sub> (alite) which can be claimed as cement components.



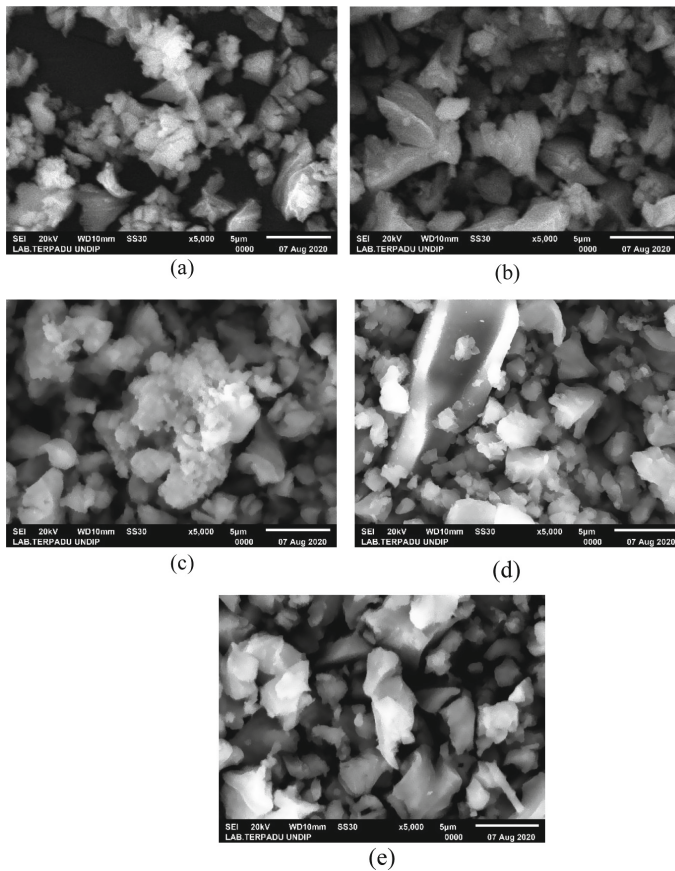


**Fig. 7.** SEM micrograph of sample 1910-950 (a), 2010-950 (b), 2110-950 (c), 2010-1000 (d), and 2010-1050 (e).

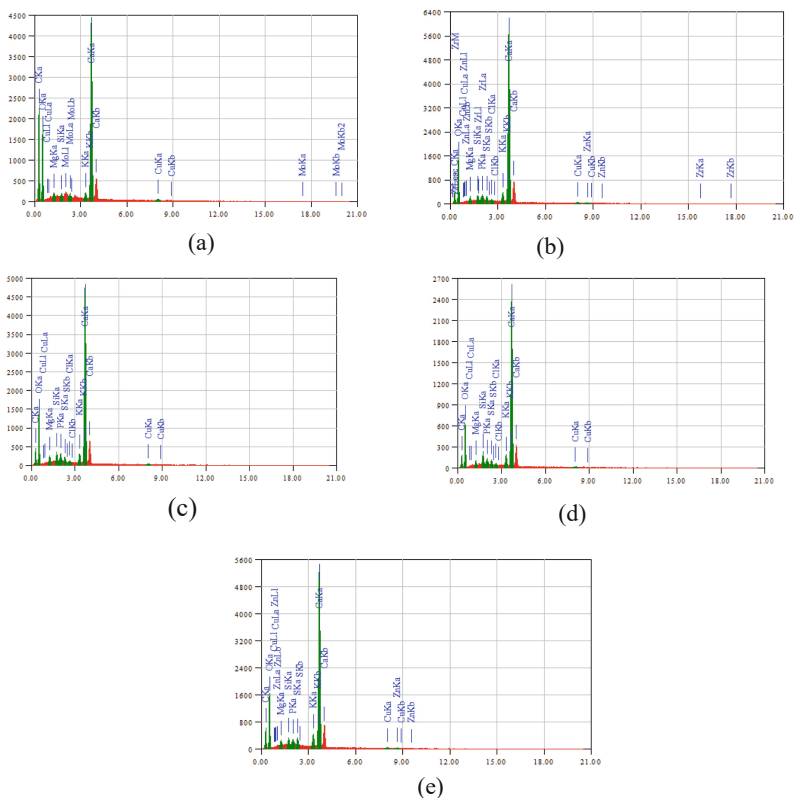


**Fig. 8.** EDX spectra of sample 1910-950 (a), 2010-950 (b), 2110-950 (c), 2010-1000 (d), and 2010-1050 (e).

**Table 3.** The elemental composition of sample 1910-950, 2010-950, 2110-950, 2010-1000, and 2010-1050.

Element	Elemental percentage (Atomic %)				
	1910950	2010950	2110950	20101000	20101050
Mg	0.21	0.64	0.75	0.55	0.53
Ca	7.04	15.76	14.00	15.03	12.87
Cu	0.23	0.30	0.34	0.20	0.25
Zr	–	0.17	–	–	–
Si	0.10	0.47	0.68	1.01	0.49
K	0.21	0.74	0.71	0.90	0.86
Mo	0.12	–	–	–	–
P	–	0.31	0.52	0.44	0.35
S	–	0.38	0.36	0.43	0.50
Cl	–	0.11	0.10	0.13	–
Zn	–	0.24	–	–	0.20

## References

- Haryono, Eddy, D. R., Noviyanti, A. R., Solihudin, & Laelaturrohmah. 2018. Kalsium Silikat sebagai Bahan Komposit Biosemen Gigi dengan Penyiapan Silika dari Sekam Padi melalui Metode Sol-Gel. *J. Kartika Kimia*. Vol 1 (2655–0938): 5–10.
- Hasibuan, R. 2016. Analisis Dampak Limbah Sampah Rumah Tangga Terhadap Pencemaran Lingkungan Hidup. *Jurnal Ilmiah "Advokasi"*. Vol 04. ISSN (2337–7216).
- Khristian, E. Pamuji. 2014. Dampak Penambangan Batu Gamping Terhadap Cadangan Air Tanah. *Penambangan Batu Gamping, Maruni, Manokwari, Papua Barat*. Vol 6 (2085–6245).
- Kriskova, L., Pontikes, Y., Zhang, F., Cizer, Ö., Jones, P. T., Van Balen, K., & Blanpain, B. 2014. Influence of Mechanical and Chemical Activation on the Hydraulic Properties of Gamma Dicalcium Silicate. *Cement and Concrete Research*. Vol 55: 59–68.
- Liu, S., Guan, X., Zhang, H., Wang, Y., & Gou, M. 2019. Revealing the Microstructure Evolution and Carbonation Hardening Mechanism of  $\beta$ -C 2 S Pastes by Backscattered Electron Images. *Materials*. Vol 19 (1561): 2–8.
- Nicoleau, L., Nonat, A., & Perrey, D. 2013. The Di- and Tricalcium Silicate Dissolutions. *Cement and Concrete Research*. Vol 47: 14–30.
- Ningsih, T., Chairunnisa, R., & Miskah, S. 2012. Pemanfaatan Bahan Additive Abu Sekam Padi pada Cement Portland. *Jurnal Teknik Kimia*. Vol 18 (4): 59–67.
- Warsy, S.Chadjiah, W. R. 2016. Telur Untuk Produksi Pasta Komposit. *Al-Kimia*. Vol 4 (2): 86–97.
- Yenny Nurchasanah. (2011). Karakteristik dan Peran Tanah Tulakan Sebagai Pozolan Alam dalam Upaya Menggantikan Semen Sebagai Bahan Konstruksi. *Seminar Nasional-I BMPTTSSI - KoNTekS 5*. Surakarta: Universitas Negeri Surakarta.

**Open Access** This chapter is licensed under the terms of the Creative Commons Attribution-NonCommercial 4.0 International License (<http://creativecommons.org/licenses/by-nc/4.0/>), which permits any noncommercial use, sharing, adaptation, distribution and reproduction in any medium or format, as long as you give appropriate credit to the original author(s) and the source, provide a link to the Creative Commons license and indicate if changes were made.

The images or other third party material in this chapter are included in the chapter's Creative Commons license, unless indicated otherwise in a credit line to the material. If material is not included in the chapter's Creative Commons license and your intended use is not permitted by statutory regulation or exceeds the permitted use, you will need to obtain permission directly from the copyright holder.

